ANNALS OF GEOPHYSICS, 67, 5, SA549, doi:10.4401/ag-9107
OPEN ACCESS

APPENDIX FOR

INDUCED GEOELECTRIC FIELD: INFLUENCE OF POLARIZATION IN COAST EFFECT AND PROXIMITY EFFECT

Giovanni Lucca[1]

[1] Retired Indipendent Reasearcher

Appendix A

The purpose of this Appendix is the derivation of Eq. (7) expressing the geoelectric field in the E polarization mode.

The thin sheet model consists of two thin layers above a common stratified basement representing the mantle of the Earth (see Fig. 1); the model comprises a conducting upper layer above a resistive layer. The first one represents the conductive crustal sediments (on the land side) or seawater (on the sea side) while the second one the resistive crust.

The thin sheet approximation is expressed, from the mathematical point of view, by the inequalities given by formulas (1); in practice, we have most of the current flowing in the conductive upper layers and the electric field is constant over this layer (with respect to z) and this produces a change in magnetic field. The values assumed by the x component of the electric field over this layer are E_{x1U} and E_{x2U} in regions 1 and 2 respectively. On the contrary, in the resistive lower layer the current is small and the magnetic field is constant over this layer (with respect to z) and instead there is a change in the electric field. The values assumed by the y component of the magnetic field over this layer are H_{y1U} and H_{y2U} respectively. See sketch in Fig. A1.

According to the 2D assumption, we have that $\vec{E} = \vec{E}(y,z)$ and $\vec{H} = \vec{H}(y,z)$ that is the electromagnetic field does not depend on the variable x. Furthermore, we are focusing only on the E polarization and, consequently, the electric field has only the x component while the magnetic field has only the y and z components.

Starting with Maxwell's equations in phasor form at low frequencies, so that the displacement current can be neglected, and with an *exp(jωt)* time dependence, we can write:

$$\frac{\partial E_x(y,z)}{\partial z} = -j\omega\mu_o H_y(y,z) \tag{A1}$$

$$\frac{\partial E_x(y,z)}{\partial y} = j\omega\mu_o H_z(y,z) \tag{A2}$$

$$\frac{\partial H_z(y,z)}{\partial y} - \frac{\partial H_y(y,z)}{\partial z} = \sigma E_x(y,z) \tag{A3}$$

$$-\frac{\partial H_z(y,z)}{\partial x} = 0 \tag{A4}$$

$$\frac{\partial H_y(y,z)}{\partial x} = 0 \tag{A5}$$

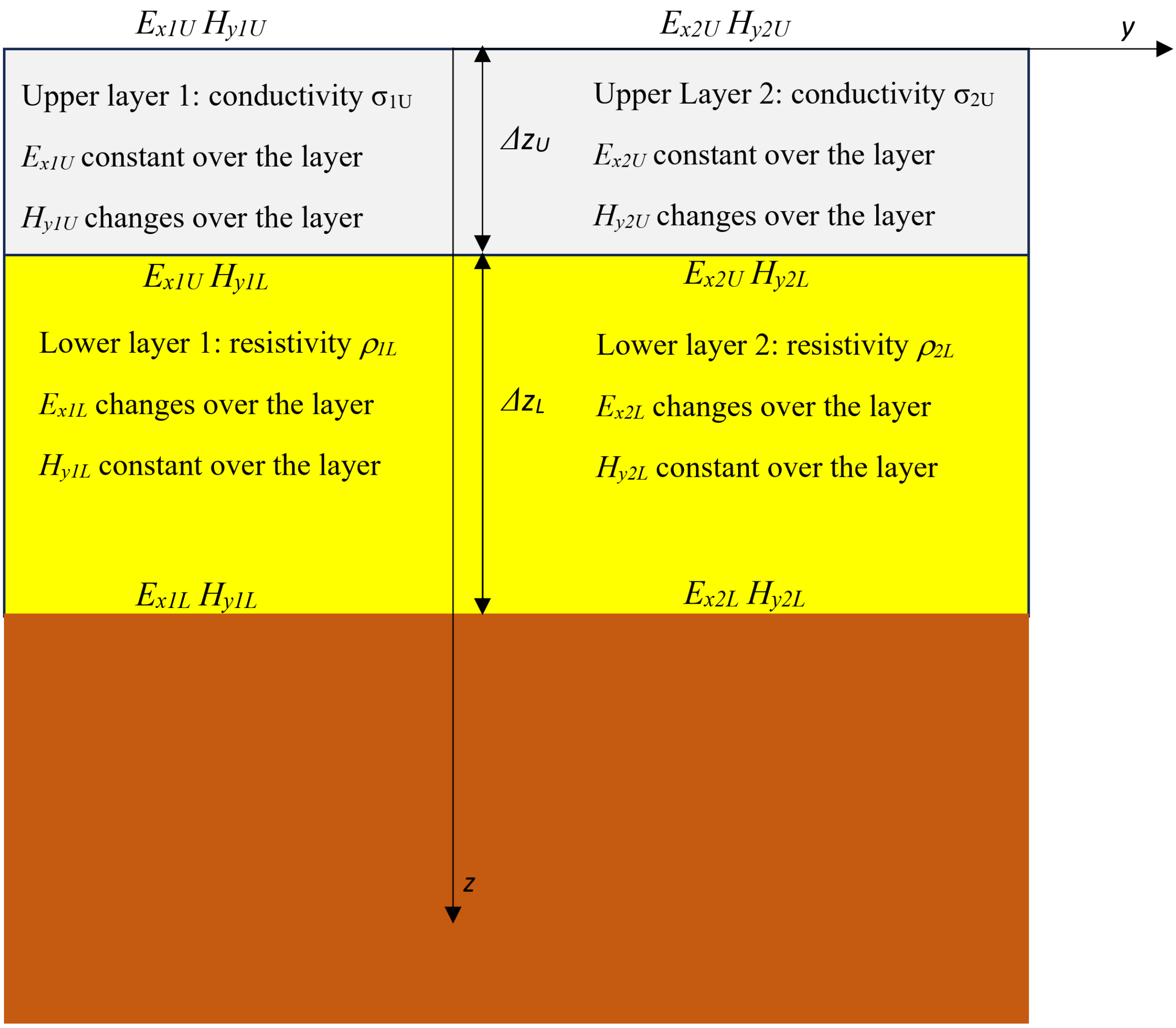

Figure A1. Sketch of the double layer thin sheet model; E_{x1U} and E_{x2U} are constant over the upper layer while H_{x1L} and H_{x2L} are constant over the lower layer.

Let us consider the second term at the left-hand side of Eq. (A3) and let us apply the thin sheet hypothesis to both the media of the upper layer; so, we can write (the quantities H_{yiL} and H_{yiU} are defined according to Fig. A1):

$$\frac{\partial H_{yiU}}{\partial z} \cong \frac{H_{yiL} - H_{yiU}}{\Delta z_{iU}} = \frac{H_{yiL} - H_{yiU}}{d_{iU}} \quad \text{(A6)}$$

We recall that the quantity d_{iU}, appearing in Eq. (A6), is defined according to Fig. 1.

By means of Eq. (A6), Eq. (A3) can be rewritten as:

$$\frac{\partial H_{ziU}}{\partial y} - \frac{H_{yiL} - H_{yiU}}{d_{iU}} \cong \sigma_{iU} E_{xiU} \quad \text{(A7)}$$

In Eq. (A7) the quantity E_{xiU} is defined according to Fig. A1.

From Eq. (A2), by differentiating with respect to y, one gets:

$$\frac{\partial H_{ziU}}{\partial y} = \frac{1}{j\omega\mu_0} \frac{\partial^2 E_{xiU}}{\partial y^2} \quad \text{(A8)}$$

By inserting it into Eq. (A7), one has:

$$\frac{d_{iU}}{j\omega\mu_0}\frac{\partial^2 E_{xiU}}{\partial y^2} - H_{yiL} + H_{yiU} - \sigma_{iU} d_{iU} E_{xiU} \cong 0 \tag{A9}$$

Let us focus now on the lower layer to get an expression for H_{yiL}.

By applying the thin sheet hypothesis, one has that, in the lower layer, the quantity H_{yiL} is constant over the whole layer itself and equal to the value assumed at the interface with the third layer; moreover, by remembering Eq. (A1), one can write:

$$H_{yiL} \cong -\frac{1}{j\omega\mu_0}\frac{E_{xiL} - E_{xiU}}{\Delta z_{iL}} = -\frac{1}{j\omega\mu_0}\frac{Z_{Ti\_3}H_{yiL} - E_{xiU}}{d_{iL}} \tag{A10}$$

Where Z_{Ti_3} is the surface impedance of the i-th medium “seen” from the interface between the second and the third layer (i.e. the interface between the crustal layers and the common basement representing the mantle shown in Fig. 1).

From Eq. (A10), we obtain:

$$H_{yiL} = \frac{E_{xiU}}{j\omega\mu_0 d_{iL} + Z_{Ti\_3}} \tag{A11}$$

By substituting Eq. (A11) into Eq. (A9) one has:

$$\frac{d_{iU}}{j\omega\mu_0}\frac{\partial^2 E_{xiU}}{\partial y^2} - \frac{E_{xiU}}{j\omega\mu_0 d_{iL} + Z_{Ti\_3}} + H_{yiU} - \sigma_{iU} d_{iU} E_{xiU} \cong 0 \tag{A12}$$

At the air-land/sea interface the magnetic field is assumed constant; so, for $z = 0$ we have, in Eq. (A12), that $H_{yiU} = H^0$. It is necessary to remark here that this assumption (adopted in some early E polarization studies e.g. Weaver (1963) is not very rigorous; nevertheless, as put into evidence by Fischer (1979), even if it represents only a first approximation, it does not completely invalidate the final result which can be seen as a first step solution of a more general scheme of successive approximations.

We also add that Dong et al., (2015b), by means of FEM and by simulating the electromagnetic field source by means of a sheet current density at the height of 100 km over Earth’s surface, shown some plots, for different frequencies, of the geomagnetic field at the Earth’s surface as a function of the distance from the coast; in proximity of the coast itself, the value of the geomagnetic field is not very different from the constant value assumed very far from it; in fact, difference is always less than 15% in absolute value.

This shows that the assumption of a constant magnetic field along the Earth’s surface has some degree of plausibility.

Furthermore, in Appendix B we compare the results obtained by applying the method here described with the results coming from FEM models by getting, overall, a fair agreement between them.

Then, for $z = 0$, Eq. (A12) becomes:

$$\frac{d^2 E_{xiU}}{dy^2} - \frac{j\omega\mu_0}{d_{iU}K_i}E_{xiU} = -\frac{j\omega\mu_0}{d_{iU}}H^0 \tag{A13}$$

Where K_i has been defined by Eq. (5).

Formula (A13) represents a non-homogeneous linear differential equation of the second order, having constant coefficients, in the unknown $E_{xiU} = E_{xiU}(y)$.

The general solution (by dropping the index U because no more necessary) is given by:

$$E_x(y,f) = \begin{cases} B_1 e^{\Gamma_1 y} + H^0 K_1 & y < 0 \\ B_2 e^{-\Gamma_2 y} + H^0 K_2 & y > 0 \end{cases} \tag{A14}$$

Where B_1 and B_2 are two constants to be determined by means of the boundary conditions at $y = 0$ and Γ_i has been defined by Eq. (6).

The boundary conditions, at $y = 0$, to be fulfilled are:

– The continuity of the tangential electric field i.e.:

$$E_{x1}(0) = E_{x1}(0) \tag{A15}$$

– The continuity of the tangential magnetic field that, by remembering Eq. (A2), is expressed by:

$$\frac{\partial E_{x1}(0)}{\partial y} = \frac{\partial E_{x1}(0)}{\partial y} \tag{A16}$$

Hence, from eqs. (A14), (A15) and (A16), one can write the following linear system in the unknowns B_1 and B_2.

$$\begin{cases} B_1 - B_2 = (K_2 - K_1)H^0 \\ B_1\Gamma_1 + B_1\Gamma = 0 \end{cases} \tag{A17}$$

The solution of system (A17) is:

$$\begin{cases} B_1 = \dfrac{H^0(K_2 - K_1)\Gamma_2}{\Gamma_2 + \Gamma_1} \\ B_2 = \dfrac{H^0(K_2 - K_1)\Gamma_1}{\Gamma_2 + \Gamma_1} \end{cases} \tag{A18}$$

Finally, by inserting the expressions for B_1 and B_2 given by Eq. (A18) into, Eq. (A14), one gets Eq. (7).

Appendix B

The purpose of this Appendix is to compare the results obtained by means of the analytical method proposed in the present paper (i.e. Eq. (7) in the case of two adjacent media with different conductivities) with the results obtained in two different publications both based on FEM approaches.

The first comparison regards the results presented by Wang and Zhang (2023) concerning the model represented in Fig. B1.

This model consists of three adjacent regions with two lateral boundaries, so we cannot directly apply Eq. (7); we have applied analogous formulas that we omit for brevity, but they can be easily obtained by generalizing the methodology here described to the case of three of more adjacent media.

The FEM model uses a uniform sheet current source parallel to the Earth's surface, having direction parallel to the two discontinuities, located at height 100 km and symmetrically spanning over the three regions; the source varies sinusoidally at a frequency 0.0001 Hz and has an amplitude of 1 A/m. The origin of the coordinate system is at the middle of the central region and the geoelectric field is evaluated as a function of the distance y from the origin; due to the symmetry of the model, the results are symmetrical with respect to z-axis.

The result of the comparison is shown in Table B1.

The second comparison regards the results presented by Dong et al. (2015) concerning the model represented in Fig. B2.

In the FEM model, the source is identical to the one adopted in the previous example but the geoelectric field is evaluated at the frequency of 0.0005 Hz.

Notice that, according model described in Fig. B2, the two layered regions on the left and on the right of the z-axis have no common basement.

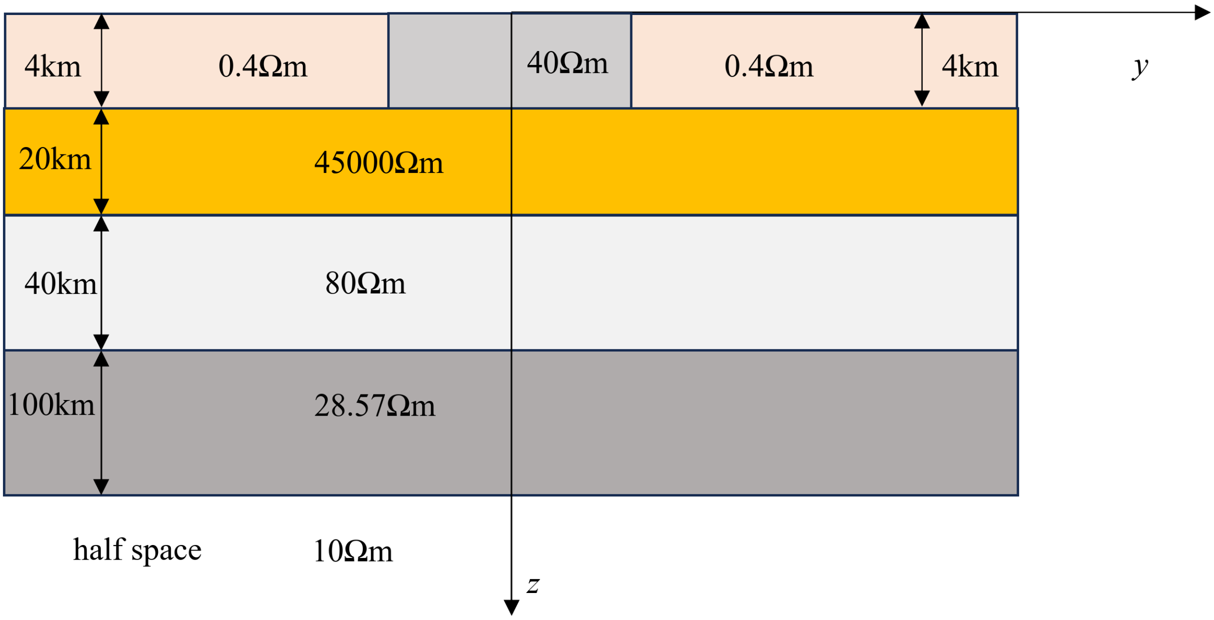

Figure B1. Model consisting of three regions with two lateral boundaries.

Distance y from the origin [km]	Geoelectric field evaluated by the method of the present paper [V/m]	Geoelectric field evaluated with FEM [V/m]
0	$1.59 \cdot 10^{-4}$	$1.53 \cdot 10^{-4}$
225	$1.59 \cdot 10^{-4}$	$1.44 \cdot 10^{-4}$
281	$1.59 \cdot 10^{-4}$	$1.41 \cdot 10^{-4}$
450	$1.47 \cdot 10^{-4}$	$1.3 \cdot 10^{-4}$
506	$1.01 \cdot 10^{-4}$	$1.14 \cdot 10^{-4}$
562	$7.28 \cdot 10^{-5}$	$1 \cdot 10^{-4}$
730	$7.1 \cdot 10^{-5}$	$9 \cdot 10^{-5}$
843	$7.1 \cdot 10^{-5}$	$8 \cdot 10^{-5}$
1067	$7.1 \cdot 10^{-5}$	$7 \cdot 10^{-5}$

Table B1. Results of the first comparison.

Table B2 show the results of the normalized geoelectric field at the Earth's surface as a function of the distance from the origin; the reference field (respect to which the field is normalized) is the one calculated in the left region of Fig. B2 at a very large distance from the xz plane separating the two half spaces.

The results of both the comparisons, certainly show some differences, but, overall, they are quite small. Therefore, the analytical formula given by Eq. (7) and its generalization to the case of more than two adjacent media is, in a first approximation, acceptable.

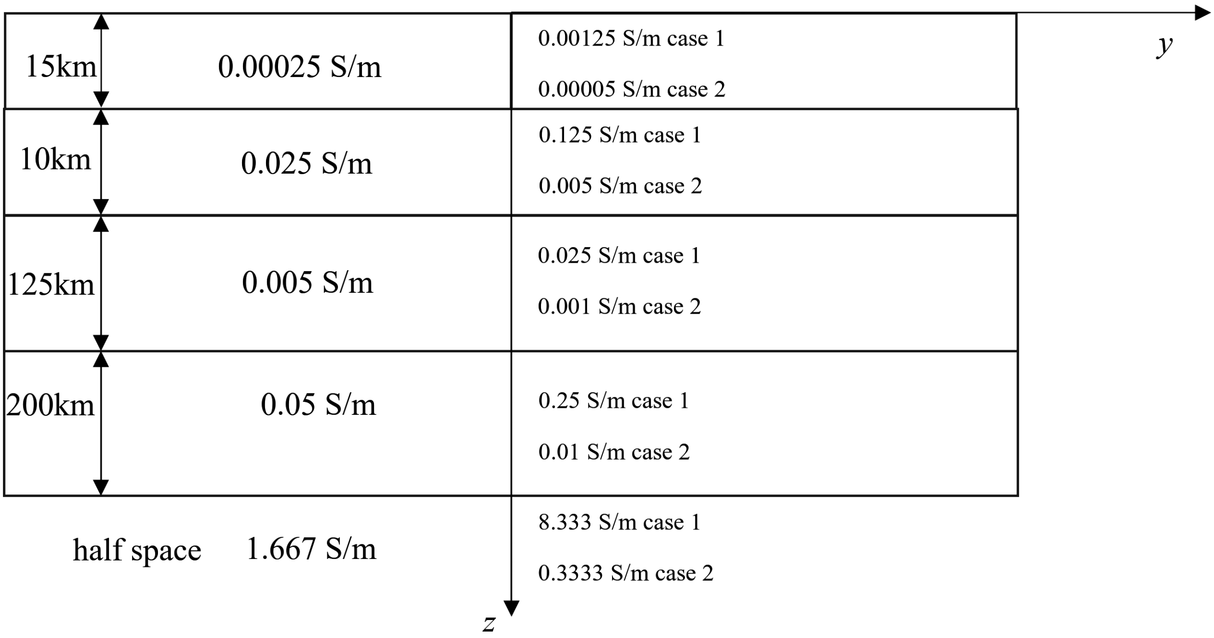

Figure B2. Model having two stratified regions separated by a common lateral boundary; it consists of two different cases depending on conductivity value assumed by the layers on the right half space while the conductivity values on the left half space are kept constant.

Distance from the origin [km]	Case 1		Case 2	
	Normalized geoelectric field evaluated by the method of the present paper	Normalized geoelectric field evaluated with FEM	Normalized geoelectric field evaluated by the method of the present paper	Normalized geoelectric field evaluated with FEM
−600	0.999	0.983	0.999	1.03
−500	0.999	0.967	0.999	1.03
−400	0.999	0.933	0.999	1.05
−300	0.998	0.917	0.999	1.067
−200	0.995	0.883	1.003	1.1
−100	0.97	0.833	1.306	1.167
0	0.808	0.75	1.271	1.25
100	0.669	0.667	1.543	1.35
200	0.655	0.583	1.602	1.43
300	0.654	0.55	1.614	1.48
400	0.654	0.533	1.616	1.53
500	0.654	0.533	1.616	1.55
600	0.654	0.533	1.616	1.57

Table B2. Results of the second comparison.